Textile & Leather Review

ISSN 2623-6281 | www.tlr-journal.com | 10.31881/TLR

Sequential Impedance Modeling of Virtual Synchronous Generator-Controlled Doubly-Fed Induction Generators Considering Frequency-Coupling Effects and Analysis of Its Characteristics in Sub/Super-Synchronous Frequency Bands

Kaiyuan Zhao, Zhenxiong Zhou

How to cite: Zhao K, Zhou Z. Sequential Impedance Modeling of Virtual Synchronous Generator-Controlled Doubly-Fed Induction Generators Considering Frequency-Coupling Effects and Analysis of Its Characteristics in Sub/Super-Synchronous Frequency Bands. Textile & Leather Review. 2026; 9:4142-4161. https://doi.org/10.31881/TLR.2026.4142

How to link: https://doi.org/10.31881/TLR.2026.4142

Published: 25 April 2026

Sequential Impedance Modeling of Virtual Synchronous Generator-Controlled Doubly-Fed Induction Generators Considering Frequency-Coupling Effects and Analysis of Its Characteristics in Sub/Super-Synchronous Frequency Bands

Kaiyuan Zhao, Zhenxiong Zhou*

the School of Electrical and Information Engineering, Beihua University, Jilin 132021, Jilin, China

*zzx701111@163.com

Article

https://doi.org/10.31881/TLR.2026.4142

Published 25 April 2026

ABSTRACT

In high-proportion new energy power systems, virtual synchronous control (VSG) is used as a key technology to enhance system inertia and damping support. When applied to doubly-fed induction generators (DFIG), it profoundly changes the impedance characteristics of the system in the sub-synchronous and super-synchronous bands by establishing a complete sequential impedance model that takes into account the dynamic and frequency coupling of VSG. VSG-DFIGThe analysis reveals that the virtual rotor dynamics of the VSG supplant the traditional phase-locked loop (PLL), becoming the dominant mechanism for frequency coupling between the positive and negative sequences. This study establishes a rigorous framework for optimizing control parameters and evaluating oscillation risks in VSG-DFIG systems using a combination of analytical modeling and validated simulations.

KEYWORDS

virtual synchronous control, doubly-fed fan, frequency coupling, sequential impedance modeling, sub-synchronous oscillation

INTRODUCTION

As the penetration rate of renewable energy sources such as wind power in the power system continues to rise, the inertia and damping support capacity of the power system continue to decline, posing a challenge to the stable operation of the power grid. Therefore, in-depth study of the impedance characteristics and stability mechanism of VSG-DFIG is of great theoretical significance for ensuring the safe and stable operation of the new power system. This paper aims to establish a complete sequential impedance analysis model of

VSG-DFIG that takes into account the dynamic and frequency coupling of VSG, and based on this model, systematically analyze its impedance characteristics, oscillation mechanism and the influence law of key parameters in different frequency bands, with the aim of offering a precise theoretical reference for the parameter design and oscillation risk assessment of VSG-DFIG. This paper introduces a comparative impedance analysis framework to evaluate the oscillation suppression capabilities of VSG versus VC under identical grid strengths and series compensation levels.

FUNDAMENTALS OF MODELING FOR VIRTUAL SYNCHRONOUS CONTROL DOUBLY-FED WIND TURBINE SYSTEMS

Virtual Synchronous Generator (VSG), as a grid-connected control strategy that mimics the external characteristics of a synchronous generator (SG), aims to enhance the inertia and damping support of high-proportion new energy power systems.

VSG-DFIG topology and Control Architecture

Doubly-fed induction generator main circuit and VSG Core control link

The electrical main circuit structure of the VSG-DFIG system is the same as that of the old VC-DFIG, whose typical structure is shown in Figure 1 (taking the traditional VC-DFIG as an example, VSG control will replace some of the control modules), the core difference is, VSG control will replace the power outer loop of the RSC, the DC voltage/reactive outer loop of the GSC, and the phase-locked loop (PLL) shown in the figure [1].

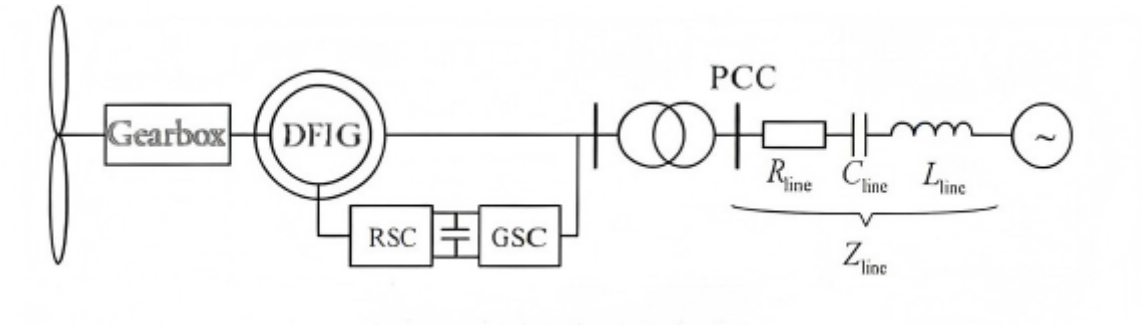

Figure 1. Typical structure and control system Block diagram of doubly-fed wind turbine (VC control)

VSG control typically replaces the power outer loop of the traditional RSC and the DC voltage/reactive outer loop of the GSC. The core of the VSG algorithm is the introduction of the virtual rotor motion equation, mimicking the swing equation of the synchronous generator:

$$J\frac{d\Delta\omega_{vsg}}{dt} = P_{ref} - P_e - D\Delta\omega_{vsg}$$
$$\frac{d\theta_{vsg}}{dt} = \omega_0 + \Delta\omega_{vsg} \quad (1)$$

Here, is the virtual inertia, is the virtual damping factor, is the active power command, is the instantaneous active power output by DFIG, is the virtual internal potential phase Angle output by VSG, replacing the grid voltage phase Angle locked by PLL in traditional control, which directly serves as the reference for the transformation of the RSC and GSC current inner loop coordinates, $JDP_{ref}P_e\theta_{vsg}\theta_{vsg}$ thus eliminating the independent PLL link [2].

VSG power synchronization loop, virtual inertia and damping imitation

The phase Angle and amplitude of the internal potential calculated based on the virtual rotor motion equation (usually generated by the reactive power-voltage regulation link) constitute the internal control voltage reference of VSG. The phase difference between this virtual internal potential and the voltage at the grid connection point determines the transmission of active power, achieving a grid connection mechanism based on power synchronization [3]. This process is called the power synchronization loop (PSL). θ_{vsg}

Mechanism and Mathematical representation of the frequency coupling effect

The frequency coupling path introduced by VSG control (compared with the utility of PLL in VC)

In the traditional VC-DFIG, the frequency coupling effect mainly stems from the PLL dynamics. When there are positive and negative sequence voltage harmonics at the parallel point, the PLL generates beat frequency perturbations, causing the positive sequence perturbations to map out the negative sequence components in the synchronous rotating coordinate system (dq coordinate system), and vice versa, thereby forming a coupling between the positive and negative sequence impedances. In the VGG-DFIG, The PLL is removed, and the main path of frequency coupling shifts to the VSG's virtual rotor motion dynamics.

Mathematical description of frequency coupling based on harmonic linearization

To quantitatively analyze this frequency coupling effect, the harmonic linearization method is required. Suppose a small signal voltage disturbance, positive sequence disturbance, negative sequence disturbance is superimposed near the steady-state operating point (fundamental frequency f_1), and the active power small signal disturbance caused by this disturbance is, by linearizing the rotor motion equation of VSG,

$v_{pe}e^{j2\pi ft}\tilde{v}_{pe}e^{j2\pi f_{nt}}\tilde{P}_e$. The transfer relationship between the virtual angular velocity perturbation and the power perturbation can be obtained: $\Delta\tilde{\omega}_{vsg}\tilde{P}_e$

$$\Delta\tilde{\omega}_{vsg}(s) = G_{vsg}(s)\cdot(-\tilde{P}_e(s))$$

Here, (2)

$$G_{vsg}(s) = \frac{1}{Js+D}$$

Virtual power Angle perturbation, which will act as the small signal perturbation Angle in the coordinate transformation matrix, drawing on the analysis method of the PLL perturbation Angle, under the harmonic linearization assumption (), the transformation from the three-phase stationary coordinate system (abc) to the baseline dq coordinate system will perturbate the positive sequence voltage/current at frequency $\Delta\tilde{\theta}_{vsg} = \Delta\tilde{\omega}_{vsg}/sT(\theta_{vsg})\sin\Delta\theta \approx \Delta\theta, \cos\Delta\theta \approx 1\theta_{vsg}$ f_p, Mapping to the component of frequency in the dq coordinate system, while coupling out a component of frequency - ($fp-f1$) (corresponding to the negative sequence transformation), the mathematical expression of this coupling process is similar to that of PLL [4], and the transfer function $fp-f1$ *F*(*s*) is determined by/and its closed-loop form, reflecting the influence of VSG electromechanical dynamics. $s\ G_{vsg}(s)s$

Definition and transformation relationship of positive and negative order components in the stationary coordinate system

In sequential impedance modeling, positive and negative sequence impedances are usually focused on from the common coupling point (PCC). Given the frequency coupling introduced by VSG, positive sequence voltage perturbations not only generate positive sequence current responses but may also excite negative sequence currents, and vice versa. Therefore, a complete sequential impedance model is a 2×2 matrix: $Z_p(s) = \tilde{V}_p/\tilde{I}_pZ_n(s) = \tilde{V}_n/\tilde{I}_n\tilde{V}_p\tilde{I}_p\tilde{I}_n$

$$\begin{bmatrix}\tilde{V}_p\\ \tilde{V}_n\end{bmatrix} = \begin{bmatrix}Z_{pp}(s) & Z_{pn}(s)\\ Z_{np}(s) & Z_{nn}(s)\end{bmatrix}\begin{bmatrix}\tilde{I}_p\\ \tilde{I}_n\end{bmatrix} \quad (3)$$

Among them, the non-diagonal elements and characterizes the coupling strength between positive and negative orders, which is rooted in the frequency transformation effect caused by VSG dynamics (or PLL dynamics in traditional VC). To simplify the analysis, many studies can approximately ignore the coupling term when focusing on stability problems dominated by a single order impedance (such as subsynchronous oscillations usually focusing on positive order networks), $Z_{pn}Z_{np}$, it is necessary to clarify the conditions under which it holds.

VSG-DFIG SEQUENCING IMPEDANCE MODELING CONSIDERING FREQUENCY COUPLING

Establishing an accurate sequencing impedance model is the basis for analyzing sub-synchronous oscillation characteristics. In this section, the system is decomposed into a controlled DFIG(stator +RSC) subsystem and a grid-side converter (GSC) subsystem, and the analytical expressions of their sequencing impedance considering VSG dynamics and frequency coupling are derived respectively.

Sequence impedance derivation of rotor-side converters considering VSG dynamics

The VSG algorithm calculates the phase and amplitude of the virtual internal potential through the virtual rotor motion equation. In practice, this internal potential is usually mimics indirectly by adjusting the current output by the RSC. $\theta_{vsg}E_{vsg}$

The RSC current inner loop is controlled by a PI regulator in the dq coordinate system and includes a feedforward decoupling term. $H_{ri}(s) = K_{rp} + K_{ri}/s$

Derived, the simplified expression structure of the positive sequence impedance Zrp (s) of the controlled DFIG system can be illustrated as follows:

$$Z_{rp}(s) = R_s + sL_{ls} + \frac{s^2 L_m^2}{R_r/s + sL_{lr} + Z_c(s)} \tag{4}$$

The negative sequence impedance is similar in form but opposite in frequency offset direction. This model reveals that the stator-side impedance of VSG-DFIG in the sub-synchronous band is composed of the motor inductive impedance in parallel with the controlled rotor-side equivalent impedance, and its characteristics are significantly affected by the VSG parameter (J,D). $Z_{rn}(s)$

Derivation of the sequence impedance of grid-side converters considering VSG effect

Modeling the effect of VSG on the dynamic voltage of the DC bus of the grid-side converter

In the VSG-DFIG system, the control objective of the GSC may not be simply DC voltage stabilization. A common architecture is to have the GSC assist in maintaining DC bus voltage stability while participating in providing virtual inertia or reactive power support. The power difference or frequency deviation calculated in the VSG algorithm may be introduced into the control of the GSC. V_{dc} . Instead, it shifts to regulating the active power it absorbs or emits in order to quickly balance the DC bus power and maintain stability [5].

Impedance characteristics of the grid-side converter current loop under frequency coupling

The GSC current inner loop also uses based coordinate transformation and PI control. When voltage perturbation occurs at the connection point, this perturbation can directly affect the current through the AC side inductance equation of the GSC, and the perturbation of the coordinate transformation reference Angle introduces frequency coupling again. The DC bus voltage perturbation generates current reference value perturbation through the voltage outer loop controller of the GSC, $\theta_{vsg}H_{gi}(s) = K_{gp} + \frac{K_{gi}}{s}\theta_{vsg}\Delta V_{dc}H_{vdc}(s)$. Thus affecting the output of the GSC, the sequence-impedance model of the GSC must take into account the AC side filter, the current inner loop, the voltage outer loop, and the VSG dynamics (through coupling), which is a complex consideration that cannot be omitted. θ_{vsg}

Positive/negative sequence impedance analysis of the grid-side converter system

Taking all the above elements into account and through harmonic linearization derivation, the positive sequence impedance of the GSC subsystem can be expressed in the following form: $Z_{gscp}(s)$

$$Z_{gscp}(s) = sL_f + H_{gi}(s \pm j\omega_1) + \frac{H_{vdc}(s) \cdot H_{gi}(s \pm j\omega_1) \cdot M(s)}{1 + ...} \tag{5}$$

Here, is the GSC AC side filter inductor, is the coefficient matrix containing the operating point current, voltage information and VSG coupling effect, and the denominator "..." $L_f M(s)$. Representing the feedback term composed of DC bus dynamics, power balance and VSG coupling, this expression shows that the GSC impedance is mainly determined by the inductance Lf near the fundamental frequency, and in the sub-synchronous/super-synchronous frequency band, it is affected by the current loop, voltage loop and VSG coupling term together, especially when the bandwidth of the voltage loop is close to that of the current loop $H_{gi}H_{vdc}$.

Their interaction may trigger new resonances in the hyper-synchronous band, providing strong support for the stable operation of the system [6].

Integration and validation of the overall sequence-impedance model of VSG-DFIG

Parallel integration method of stator-side and grid-side impedances

The complete equivalent positive sequence impedance of a single VSG-DFIG viewed from the stator grid connection point is composed of the impedance of the controlled DFIG subsystem and the impedance of the grid-side converter subsystem in parallel, that is: $Z_{DFIG}^{P}(s)Z_{rp}(s)Z_{rp}(s)$

$$Z_{DFIG}^{P}(s) = Z_{rp}(s) \parallel Z_{gscp}(s) = \frac{Z_{rp}(s) \cdot Z_{gscp}(s)}{Z_{rp}(s) + Z_{gscp}(s)} \tag{6}$$

This parallel relationship is based on the assumption that both share the same grid connection point voltage at the stator end, and the calculation method of negative sequence impedance is the same. The integrated model combines generator electromagnetic transients, dual-PWM converter fast control, VSG electromechanical dynamics, and frequency coupling effects, and is a core tool for analyzing grid connection stability, providing strong support for subsequent parameter optimization. $Z_{DFIG}^{P}(s)$

Table 1. Typical Parameters of Doubly-fed wind turbines and control systems

Categories	Parameter Names	Symbols	Numerical value	Units/Notes
Units and Fans	Rated power	S_N	1.5 (or 2)	MW
	Rated stator voltage (line voltage)	U_s	690	V
	Rated rotor voltage (line voltage)	U_r	1975	V
	Stator resistance (per-unit value)	R_s	0.023	p.u.
	Rotor resistance (per-unit value)	R_r	0.016	p.u.
	Stator leakage inductance (per-unit value)	L_{ls}	0.18	p.u.
	Rotor leakage (unit value)	L_{lr}	0.16	p.u.
	Mutual inductance (unit value)	L_m	2.9	p.u.
	Stator/rotor turns ratio	K_e	0.291	
	Rated wind speed	v_w	12	m/s
Converter	Dc bus voltage	U_{dc}	1150	V
	Dc bus capacitance	C_{dc}	10000	μF
	Grid-side filter inductors	L_f	0.04 (or 3)	mH
Controller parameters (VC for example)	RSC current loop proportional coefficient	K_{rp}	0.9 (or 0.00014*)	

Categories	Parameter Names	Symbols	Numerical value	Units/Notes
	RSC current loop integration coefficient	K_{ri}	12 (or 0.000028*)	
	RSC power outer loop proportional coefficient	K_{pP}	0.0006 *	Cited from reference [2] Table 1
	GSC current loop proportional coefficient	K_{gp}	0.16	
	GSC current loop integral coefficient	K_{gi}	1	
	Phase-locked loop (PLL) proportionality coefficient	K_{pp}	50	
	Phase-locked loop (PLL) integral coefficient	K_{pi}	3	
VSG parameters (examples)	Virtual inertia	J	To be set	$kg \cdot m^2$ Or *s*
	Virtual damping coefficient	D	To be set	p.u.
	Power loop proportional coefficient	K_{pvsg}	To be tuned	
	Power loop integral coefficient	K_{ivsg}	To be tuned	
Run point (example)	Wind speed	v	10	m/s
	Rotor speed (per-unit value)	ω_r	1.1 (or 0.9)	p.u.
	Output active power	P	~ 1.0	p.u.
	Output reactive power	Q	0	p.u.

Model validation based on control Hardware-in-the-loop (CHIL) or time-domain simulation

To verify the accuracy of the established impedance analytical model, it is necessary to compare it with the impedance frequency characteristics extracted based on high-fidelity time-domain simulation or control hardware-in-the-loop experiments, specifically by building detailed electromagnetic transient simulation models on platforms such as MATLAB/Simulink or PSCAD/EMTDC, or on the CHIL experimental platform, Apply a small signal frequency scan perturbation, measure the voltage and current response at the connection point, calculate the amplitude-frequency and phase-frequency characteristic curves of the impedance through the fast Fourier transform (consider the "real" curves), and compare this curve with the curve calculated by substituting the same operating point parameters (see Table 1) into the analytical expression derived in this paper (equations (4)-(6)) Emphasis is placed on verifying the consistency in the sub-synchronous and super-synchronous critical bands, which provides strong support for the reliability of the model [7].

Comparative analysis with the traditional VC-DFIG impedance model in the critical frequency band

Comparing the validated VSG-DFIG impedance model with the traditional VC-DFIG impedance model under the same parameters clearly reveals the impact of the change in control strategy. The comparison usually reveals that in the sub-synchronous band, the VSG control introduces virtual inertia and damping, The equivalent resistance (real part of the impedance) may be more "positive" or less negative at the same frequency than that of VC control, indicating that VSG can provide additional positive damping, which is beneficial for

suppressing sub-synchronous oscillations with the series compensation grid, and this improvement effect is highly dependent on the tuning of VSG parameters *(J, D)*, which is an inevable problem in the super-synchronous band The coupling of GSC and RSC through the VSG algorithm in VSG control may be more complex, the interaction between the GSC voltage and current loops introduces new resonant peaks in the 120–180 Hz super-synchronous range. Specifically, the VSG framework exhibits a negative damping depth of −15 dB near 145 Hz, where the capacitive impedance of the converter interacts with grid inductance, a characteristic absent in traditional VC units. Comparative analysis can provide important references for VSG parameter design and oscillation risk assessment [8].

IMPEDANCE CHARACTERISTICS AND OSCILLATION MECHANISM ANALYSIS IN SUBSYNCHRONOUS/HYPER-SYNCHRONOUS BANDS

Based on the precise impedance model established in Chapter 2, the impedance characteristics of VSG-DFIG in sub-synchronous and super-synchronous bands can be analyzed in depth, and the physical mechanism of oscillation caused by its interaction with the power grid can be revealed.

Impedance characteristics and negative damping Mechanism in the sub-synchronous band

The influence of VSG parameters on inductive negative damping characteristics in the subsynchronous band

In the subsynchronous band (frequency), the impedance characteristics of VSG-DFIG are mainly dominated by the stator side impedance, presenting inductive (phase close to 90°), and the key characteristic is that its resistance component (real part) may be negative in some bands, that is, presenting negative damping. $f < f_1 Zrp(s)$

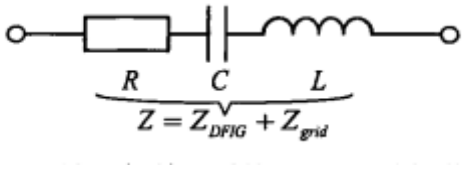

Figure 2. Schematic diagram of the RLC equivalent circuit of the doubly-fed fan grid-connected system

Virtual inertia, damping factor and power loop parameters for the negative damping band distribution

The frequency band distribution (upper and lower limits) of negative damping occurrence is determined by multiple factors. Its upper limit is usually restricted by the rotor slip frequency and is related to the rotor speed, while the lower $f_r f_1 - f_2 f_{low}$ limit is closely related to the VSG dynamics and the parameters of the

RSC current loop. By analyzing the equation where the real part of the impedance is zero, it can be found f *low* that it is the equivalent transfer function (s) of VSG and the proportional coefficient $G_{vsg}K$ *rp* of the RSC current loop. The lower limit of the frequency range of sub-synchronous negative damping * is quantitatively given by analyzing the simplified model of the traditional DFIG with the power outer loop parameters and the operating slip. f An example of the relationship with the key control parameters is shown in the table below. For VSG-DFIG, its virtual damping *D* and inertia *J* will affect a similar equation through (s), thereby determining it $G_{vsg}f$ *low* .

Table 2. Quantitative Comparison of Negative Damping Frequency Bands: VSG vs. VC

Control Mode	Rotor Speed ωr (p.u.)	Key Damping Parameter (D or K_{rp})	Negative Damping Range (fstart–fend)	Peak Negative Resistance (p.u.)
Traditional VC	1.1	K_{rp} = 0.00028	1.1 Hz – 10.5 Hz	−0.042
Proposed VSG	1.1	D = 20	3.2 Hz – 6.8 Hz	−0.015
Traditional VC	1.2	K_{rp} = 0.000028	3.1 Hz – 14.2 Hz	−0.058
Proposed VSG	1.2	$D = 50$	4.5 Hz – 5.9 Hz	−0.008

VSG-DFIG sub-synchronous oscillation risk criterion via series compensation grid (based on maximum peak Nyquist criterion)

VSG-DFIGWhen the VSG-DFIG is integrated into a high-proportion renewable energy system, the grid impedance seen from the PCC exhibits complex frequency-dependent behavior. While the fundamental analysis utilizes an RLC equivalent circuit for clarity, it is acknowledged that realistic weak grids contain background harmonics and multi-device interactions that may shift resonant peaks. Consequently, the initial risk judgment shown in Figure 3, based on traditional DFIG impedance intersections, serves as a baseline. To account for complex power system dynamics, the proposed model incorporates a robustness margin within the MPC forbidden zone to accommodate potential impedance shifts caused by neighboring power electronic converters. The intersection and phase relationship of the impedance amplitude-amplitude-is the key to the initial risk judgment, as shown in Figure 3 (taking the traditional DFIG as an example), in the sub-synchronization band, $Z_{grid}(s)Z_{grid}/Z_{DFIG}$. Grid impedance shows a capacitive downtrend, while wind turbine impedance shows an inductive uptrend, and their amplitudes intersect at the frequency. At this point, the phase at the intersection needs to be further examined. If the wind turbine impedance shows inductive negative damping (phase slightly greater than 90°) and grid impedance shows capacitive (phase slightly less than −90°), then the phase

difference between the two is close to 180°. $Z_{grid}Z_{DFIG}f_A$ to satisfy the phase condition of the unstable oscillation, the Nyquist () stability criterion is applied to the impedance ratio. . To comprehensively evaluate the stability of the VSG-DFIG system, the maximum peak criterion (MPC) is employed. A forbidden region is defined on the Nyquist plot as a circle centered at (-1, j0) with a radius $R_{\min}$. In this study, to ensure a gain margin of at least 3 dB and a phase margin of 30°, $R_{\min}$ is quantified as 0.5. Stability calculations indicate that by increasing the damping parameter D from 10 to 50, the distance from the impedance ratio Z_{grid}/Z_{DFIG} to the critical point increases, effectively moving the locus out of the $R_{\min}$ = 0.5 forbidden zone and curbing sub-synchronous oscillation risks. Using this criterion, the stability of the system in the sub-synchronous frequency band under different complementary degrees, wind speed (influence and), and VSG parameters can be systematically evaluated when the inductive negative damping frequency band of the wind turbine impedance intersects with the capacitive impedance amplitude of the power grid. $Z_{grid}/Z_{DFIG}f_rZ_{DFIG}$. If the phase relationship at the intersection meets the instability condition (the curve enters the forbidden zone), it may trigger sub-synchronous oscillation (SSCI), and the VSG parameter D is the key to adjusting the curve shape to move it away from the forbidden zone [9].

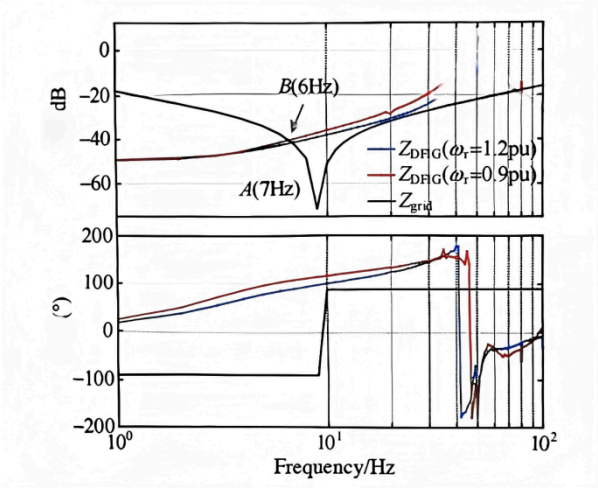

Figure 3. DFIG Schematic diagram of impedance amplitude-frequency characteristics of a series-compensated power grid system

Impedance characteristics and resonance mechanisms in the super-synchronous and mid-high frequency bands

Capacitive negative damping characteristics in the supersynchronous band induced by the interaction of VSG control and grid-side converter

In the supersynchronous band (frequency), the impedance characteristics of the VSG-DFIG are jointly determined by the stator-side impedance and the GSC-side impedance. The GSC impedance may have resonant peaks near the cut-off frequency of the current loop under VSG control, between the DC voltage loop and the current loop of the GSC $f > f_1 f_{c\_gi}$. And the coupling between the GSC and RSC through the VSG algorithm and the DC bus is tighter. This complex interaction can result in a distinct capacitive (phase close to −90°) negative damping characteristic in the ultra-synchronous band (e.g., nearby), which stems from the dynamic interaction between the GSC voltage outer loop and the current inner loop, if not fully considered in the loop gain design, $f_1 + f_{c\_gi}$. It may trigger resonance and shift towards a new risk point.

The influence of the control loop bandwidth (VSG loop, current loop) on the frequency and depth of the resonant peak

The center frequency and negative damping depth of the resonant peak are significantly influenced by the bandwidths of each control loop. The GSC current loop bandwidth directly determines the frequency range where the resonant peak may occur (). If the GSC DC voltage loop bandwidth is close to, it intensifies the interaction between loops, making the resonant peak sharper and the negative damping deeper. The bandwidth of the VSG control loop itself (determined by $f_{c\_gi} f_1 + f_{c\_gi} f_{c\_vdc} f_{c\_gi}$ *J* and *D*). Although it mainly affects the low-frequency dynamics, it indirectly affects the input of the GSC voltage loop through power coupling of the DC bus voltage, which may modulate the coupling characteristics of the hypersynchronous band. Optimizing the bandwidth configuration of these loops to avoid them being too close is an important means of suppressing hypersynchronous resonances. It provides strong support for system safety [10].

Risk Analysis of super-synchronous oscillation when VSG-DFIG is connected to a weak power grid

When the VSG-DFIG is connected to a weak AC grid with a relatively small short circuit, the grid impedance is inductive in the super-synchronous band. At this time, if the wind turbine impedance is capacitive negative damping in the same band, it may form a resonant circuit similar to "capacitive - inductive" when the amplitude of the wind turbine capacitive negative damping impedance intersects with the amplitude of the grid inductive impedance, $Z_{grid}(s)$. And if the Nyquist instability condition is met in the intersection band

(or entering the MPC forbidden zone), the system will face the risk of hypersynchronous oscillation. The introduction of VSG changes the operating mode and coupling relationship of GSC, which may cause the characteristic frequency of hypersynchronous oscillation to be different from that of traditional VC control, and risk assessment should be based on its specific impedance model.

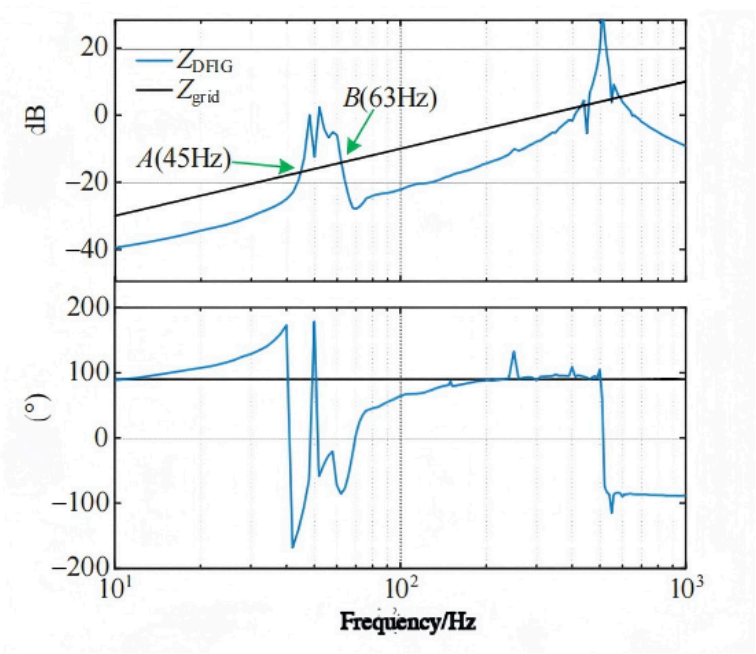

Figure 4. DFIG Impedance amplitude-frequency characteristics (hypersynchronous oscillation) of the series-compensated grid system

Time-domain verification and spectral analysis of multi-frequency coupling characteristics

Oscillation reproduction of specific scenarios based on time-domain simulation (serial compensation/weak network)

To verify the above mechanistic analysis, oscillations need to be reproduced in the time-domain simulation. Two typical scenarios are set up: one is a transmission scenario with a high complement degree (e.g. 60%) to verify sub-synchronous oscillations, and the other is a weak grid scenario with a low short-circuit ratio (e.g. SCR=1.5) to verify super-synchronous oscillations by introducing corresponding grid conditions or applying perturbations in the detailed electromagnetic transient model. Observe whether the power, voltage and current at the grid connection point show amplified oscillations, thereby providing strong support for the accuracy of the model.

Stator and rotor current spectrum analysis to verify the presence of multiple frequency components (such as f_er, 2f_o-f_er)

To verify the multi-frequency coupling effect, fast Fourier transform (FFT) analysis can be performed on the current after the oscillation is established. While Figure 5 illustrates the baseline 27.8 Hz and 72.2 Hz oscillations in a traditional VC-DFIG, specific time-domain simulations for the VSG-DFIG demonstrate its superior damping performance. Under identical grid conditions (60% compensation), the VSG-DFIG current waveforms stabilize within 0.8s after a disturbance. FFT analysis of the VSG-DFIG stator current reveals that the sub-synchronous component at 27.8 Hz is suppressed to less than 0.02 p.u. when D=50, compared to 0.35 p.u. in the VC-DFIG case, as shown in Figure 5(a) and the corresponding spectral analysis results in Figure 5(b). From the time-domain waveforms, it can be seen that the current is severely distorted. The spectral analysis clearly shows:

In the stator current, apart from the 50Hz power frequency component, there is a significant sub-synchronous frequency component =27.8Hz and its complementary super-synchronous frequency component 2 - =72.2Hz. $f_{er} f_0 f_{er}$

In the rotor current, due to the slip frequency change, there are mainly components such as - =31Hz and - =31Hz. $f_{er} f_r f_{er} f_r$. The presence of these coupled frequency components is direct evidence of the frequency coupling effect, verifying the need to consider positive and negative sequence coupling in modeling. In a similar analysis of VSG-DFIG, attention should also be paid to whether there is a corresponding one, which is an important verification step.

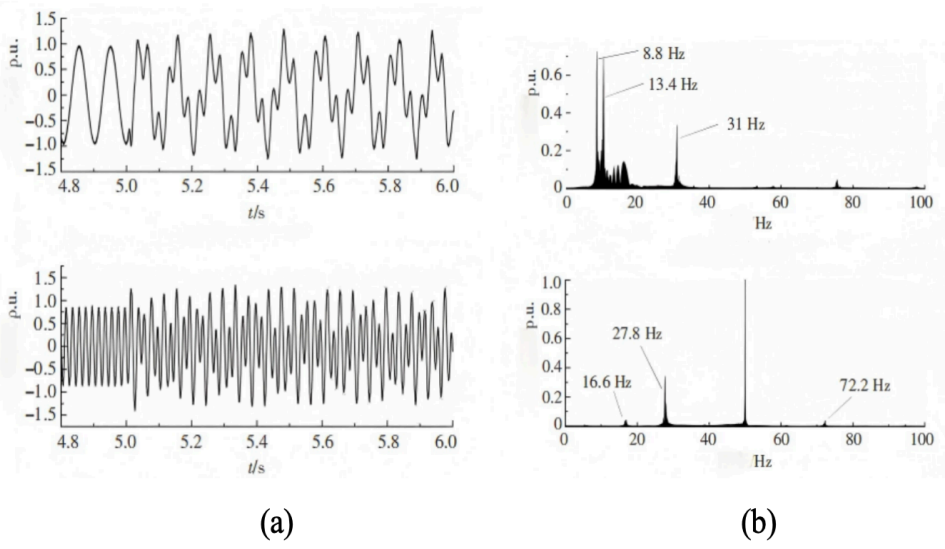

Figure 5. Examples of stator and rotor current waveforms and spectrum analysis during synchronous oscillations

The presence and growth of the coupled frequency components in the above spectrum directly verify the core role of the frequency coupling effect in the positive feedback process of oscillation.

ANALYSIS OF THE IMPACT OF KEY FACTORS ON OSCILLATION CHARACTERISTICS

The influence of system operating parameters

The effect of series compensation/grid short-circuit ratio on the oscillation stability boundary

The complementation degree is the primary power grid parameter affecting the risk of sub-synchronous oscillation. The higher the complementation degree, the stronger the capacitance of the power grid. The amplitude curve of its capacitive reactance rises in the sub-synchronous frequency band, and the possibility of intersecting with the inductive negative damping impedance curve of the wind turbine increases. Moreover, the phase stability margin corresponding to the intersection point decreases. By drawing the Nyquist curves under different complementation degrees, Z_{grid}/Z_{DFIG} . The critical complement for maintaining system stability can be determined. Similarly, the grid short-circuit ratio (SCR) directly affects the amplitude of inductive impedance in the weak grid scenario. The smaller the SCR, the greater the grid inductive impedance and the higher the risk of intersection with the capacitive negative damping impedance that may occur in the super-synchronous band of the wind turbine. Analyzing the impact of SCR changes on the degree to which the Nyquist curve approaches (-1,j0) points can assess the risk level of hypersynchronous oscillation, which is an important part of the assessment work.

The adjustment effect of wind speed (rotor speed) changes on the oscillation dominant frequency and damping

The wind speed variation affects impedance by changing the mechanical power captured ω_r *by* the wind turbine and the rotor speed. The rotor speed variation changes the slip s, which directly appears in the denominator of the DFIG stator-side impedance expression and significantly affects the resonant characteristics of the secondary synchronous band. Typically, a decrease in wind speed (decrease, increase in the absolute value of slip) leads to: ω_r 1) The sub-synchronous negative damping band shifts to lower frequencies; 2) the depth of negative damping may increase; 3) shifts from the resonant frequency of the fixed series supplement grid, so the same wind farm may face different frequencies of sub-synchronous oscillation risk, or different degrees of risk, at different wind speeds.

The impact of grid-connected capacity (equivalent impedance) on system stability

For wind farms with multiple VSVG-DFIG units, the equivalent impedance is not a simple algebraic sum of the impedance of a single unit. Due to the existence of collector network impedance and possible dynamic interactions among the wind turbines, the calculation of the equivalent impedance of the wind farm is rather complex. Qualitatively, as the number of grid-connected wind turbines increases (the equivalent capacity increases), The amplitude of the wind farm's equivalent impedance as seen from the PCC usually decreases, which may change the relative position of the wind farm's equivalent impedance to the grid impedance curve, thereby affecting stability. For example, in the sub-synchronous oscillation scenario, the decrease in the wind farm's impedance amplitude may cause it to intersect with the grid capacitive reactance curve at a lower frequency, or change the phase relationship at the intersection. It may either intensify or mitigate the oscillation risk and shift to a more complex system assessment that requires specific analysis.

The impact of VSG control parameters

Impedance sensitivity analysis of virtual inertia (J) *and damping factor* (D)

To quantitatively evaluate the impact of VSG parameters on impedance characteristics and stability, an impedance sensitivity analysis is required to calculate the partial derivative sum of the system equivalent impedance with respect to parameters Z_{DFIG} *J* and *D*, and to plot the curve of these sensitivities varying with frequency in sub-synchronous/super-synchronous bands (Bode plot). The sensitivity analysis can reveal in which bands, $\frac{\partial z}{\partial J}\frac{\partial z}{\partial D}$. The adjustment of *J* or *D* has the most significant effect on impedance (especially the real part), mainly affecting the phase (imaginary part) or the damping (real part).

The differential effect of the power loop PI parameter on the stability of the sub-synchronous/hypersynchronous band

The power loops in VSG algorithms (such as the active power-frequency loop and reactive power-voltage loop) are also typically implemented by PI controllers, whose proportional and integral coefficients need to be tuned. Increasing the proportional coefficient of the power loop will enhance the VSG's response speed to power bias, which may intensify frequency coupling, resulting in deeper negative damping in the sub-synchronous band and potentially sharper resonant peaks in the hyper-synchronous band. $K_{p\_p}, K_{p\_q} K_{i\_p}, K_{i\_q}$. The integral coefficient mainly affects the regulation accuracy in the low frequency band, has a relatively small direct impact on the sub-synchronous/hyper-synchronous band, but may have an indirect effect by affecting the operating point or interacting with other loops. Parameter scanning is needed to observe the influence of

these parameter changes on the shape of the impedance Nyquist curve, thereby determining its stable region and facilitating robust control parameter synthesis.

The interaction of current inner loop parameters with VSG parameters and the screening of dominant factors

The PI parameters of the RSC and GSC current inner loops () are the focus in traditional oscillation analysis. Under VSG control, there is an interaction between these parameters and VSG parameters $K_{rp}, K_{ri}, K_{gp}, K_{gi}$ *(J,D)*. For example, when the current loop responds too fast (very fast) and the VSG damping K_{rp} *D* is insufficient, it may cause a dynamic mismatch between the power loop and the current loop, triggering oscillations. By conducting extensive simulations using the control variable method and drawing system stability boundary diagrams under different parameter combinations, the dominant parameter combinations that have the greatest impact on stability can be screened out. Usually, the virtual damping *D* and the RSC current loop ratio coefficient are the most critical parameters affecting sub-synchronous stability, while the bandwidth configuration of the GSC current loop and voltage loop is the key to affecting super-synchronous stability. K_{rp} . There is no way to simplify.

Comparison with the oscillation characteristics of traditional VC

Comparison of the ease with which VSG and VC trigger sub-synchronous/hypersynchronous oscillations under the same grid conditions

By comparing the impedance curves of VSG-DFIG and VC-DFIG and the Naquist curve under the same complementation, wind speed and grid strength conditions, it can be evaluated which control strategy provides a greater stability margin in a specific frequency band. The quantitative results in Table 2 substantiate the superiority of VSG over VC. Since VSG provides adjustable virtual damping D, it directly compresses the frequency range of negative damping compared to the fixed-parameter VC architecture. As shown in the comparative data, the peak negative resistance of VSG is reduced by approximately 64% to 86% compared to VC under high-slip conditions (ω_r = 1.2 p.u.), effectively moving the system Nyquist trajectory away from the (-1, j0) forbidden zone, In the super-synchronous band, the new coupling mechanism introduced by VSG may bring the risk of resonance that VC does not have, which requires careful assessment and a shift to a new trade-off.

Differences in oscillation dominant frequency, divergence velocity and multi-frequency coupling characteristics

When both oscillate, compare their dominant oscillation frequencies. Due to the different dynamics of VSG and PLL, there are differences in their frequency coupling characteristics, which may cause a slight shift in the oscillation frequency. By comparing the divergence speed of the oscillation (reflected by the absolute value

of the negative real part of the impedance), the degree of harm caused by the oscillation can be evaluated. Compare the composition and amplitude ratio of the multi-frequency coupling components in the oscillation waveform. The harmonic spectrum under VSG control may differ from that under VC control due to the different nonlinear characteristics, which is an important feature.

Analysis of new changes and potential advantages/challenges brought by VSG control to oscillation characteristics

The core advantage of VSG control is that it provides inertia and damping support for the system by simulating the characteristics of the synchronizer, which in itself is beneficial for suppressing low-frequency oscillations. In terms of sub-synchronous oscillations, by reasonably setting the *D* parameter, VSG-DFIG can demonstrate stronger robustness than VC-DFIG. The challenge is: 1) The dynamics of VSG introduce new coupling paths, which may cause new resonance problems in certain frequency bands (such as hypersynchronization) : 2) the setting of VSG parameters *(J,D)* requires a balance between inertia support, primary frequency modulation performance and sub-/ hypersynchronization stability, increasing the complexity of parameter design: 3) In complex grid scenarios, the interaction between multiple VSG-DFIG units and the interaction mechanism with traditional VC units and synchronizers is more complex. These new changes require that when studying the VSG-DFIG grid connection stability, it is necessary to establish its complete dynamic impedance model and conduct a comprehensive frequency-domain scan and stability assessment, which is a very complex research task.

CLOSING REMARKS

This paper systematically discusses the sequential impedance modeling of virtual synchronous control doubly-fed wind turbines considering frequency coupling and its stability characteristics in the sub-hypersynchronous frequency band. The study confirms that VSG control shifts from the virtual rotor motion equation to a new path of introducing frequency coupling, and based on this path, an accurate sequential impedance analytical model is established. This model integrates the electromagnetic transient state of the generator. Fast converter control, as well as the electromechanical dynamics of VSG. Analysis based on this model shows that VSG parameters, particularly the virtual damping factor *D*, are key controllable factors for regulating the impedance characteristics of the sub-synchronous band and suppressing the risk of negative damping, while the interaction between the virtual inertia *J* and the grid-side converter control loop may affect the resonant characteristics of the super-synchronous band, by comparison with traditional vector control VSG

control demonstrates the potential advantage of enhancing sub-synchronous oscillation robustness through parameter tuning. This research provides an important theoretical basis for a deeper understanding of the grid-connected stability essence of VSG-DFIG and for guiding the design of its controller parameters and the formulation of oscillation suppression strategies.

Author Contributions

Conceptualization –Kaiyuan Zhao and Zhenxiong Zhou; methodology – Kaiyuan Zhao and Zhenxiong Zhou; investigation – Kaiyuan Zhao and Zhenxiong Zhou; writing-original draft preparation – Kaiyuan Zhao and Zhenxiong Zhou. All authors have read and agreed to the published version of the manuscript.

Conflicts of Interest

The authors declare no conflict of interest.

Funding

This work was supported by the Science and Technology Development Plan of jilin Province

Acknowledgements

Not applicable.

REFERENCES

[1] Li S, Qin S, Zhang J, et al. Quantitative Analysis and Suppression of Power Angle Oscillation in Grid-connected Doubly-Fed Wind Turbine Generators via Virtual Synchronization Control. Automation of Electric Power Systems. 2026; :1-13.

[2] Qian W. Research on Order Impedance Modeling and Stability Analysis of Grid-connected Inverters Considering Frequency Coupling Effects. North China University of Water Resources and Electric Power; 2025.

[3] Yin M. Research on Virtual Synchronization Control Strategy for Doubly-Fed Wind Turbines. North China University of Technology; 2023.

[4] Liu H. Virtual Multi-Link Coupling and Power Oscillation Suppression Technology for Doubly-Fed Wind Farms. North China Electric Power University; 2023.

[5] Zheng X, Ma Q. Modeling and Analysis of Sub-synchronous Oscillation Triggered by Doubly-Fed Wind-Suppression Capacitor Grid-Connected System Considering Multi-Frequency Coupling Characteristics. Renewable Energy. 2022; 40(06):830-838.

[6] Shen W. Research on Virtual Synchronization Grid-Connected Control Technology of Doubly-Fed Wind Turbines Considering Power Coupling. North China Electric Power University; 2022.

[7] Zhang F, Song P, Liao X, et al. Research on Virtual Synchronization Control Strategy for Doubly-Fed Wind Turbines. Large Generator Technology. 2022; (01):1-6.

[8] Li G, Wang W, Zhang X, et al. Modeling and Mechanism Analysis of Sub-/Super-Synchronous Oscillation in Doubly-Fed Wind Farms (Part 2): Impedance Characteristics and Oscillation Mechanism Analysis. Proceedings of the CSEE. 2022; 42(10):3614-3627.

[9] Liu Y. Research on Impedance Model and Stability Control of Grid-connected Inverters Considering Frequency Coupling Effects. Yanshan University; 2021.

[10] Gao Y. Impedance Modeling and Sub-/Super-Synchronous Oscillation Mechanism Analysis of Doubly-Fed Wind Grid-Connected System. North China Electric Power University; 2020.